Rapid Communication

Characterization of relativistic electrons generated by a cone guiding laser pulse*

Liu Hong-Jie(刘红杰)[a)b)], Gu Yu-Qiu(谷渝秋)[a)b)†], Zhou Wei-Min(周维民)[a)], Yu Jin-Qing(余金清)[a)], Zhu Bin(朱 斌)[a)], Wu Yu-Chi(吴玉迟)[a)], Shan Lian-Qiang(单连强)[a)], Wen Xian-Lun(温贤伦)[a)], Li Fang(李 芳)[a)], Qian Feng(钱 凤)[a)c)], Cao Lei-Feng(曹磊峰)[a)b)], Zhang Bao-Han(张保汉)[a)b)], and Zheng Zhi-Jian(郑志坚)[a)b)]

[a)] *Laser Fusion Research Center, China Academy of Engineering Physics, Mianyang* 621900, *China*

[b)] *National Key Laboratory of Plasma Physics, Mianyang* 621900, *China*

[c)] *College of Optoelectronic Engineering, Chongqing University, Chongqing* 400044, *China*

(Received 5 September 2011; revised manuscript received 14 October 2011)

We demonstrated the interaction of a gold cone target with a femto second (fs) laser pulse above the relativistic intensity of 1.37×10^{18} μm^{2}W/cm^2. Relativistic electrons with energy above 2 MeV were observed. A 25%–40% increase of the electron temperature is achieved compared to the case when a plane gold target is used. The electron temperature increase results from the guiding of the laser beam at the tip and the intense quasistatic magnetic field in the cone geometry. The behavior of the relativistic electrons is verified in our 2D-PIC simulations.

Keywords: relativistic electrons, gold cone, guiding laser, electron temperature

PACS: 52.57.–z, 52.38.–r, 41.75.–i **DOI:** 10.1088/1674-1056/21/5/055207

1. Introduction

The interaction of high intensity short pulse lasers with solid targets has been of increasing interest in recent years. The most studied application is fast ignition and X-ray source generation.[1−10] In the fast ignition (FI) scheme of inertial confinement fusion (ICF), the deuterium-tritium fuel capsule is first compressed to high density by long-pulse lasers.[11] A short intense laser pulse then produces an energetic electron beam to ignite the dense core. The realization of the fast ignition concept is challenging since the core is hidden under a plasma corona with a long scale length.[6,9] It is very difficult for laser pulse to get to the dense core. Thereby, a hollow cone is proposed to attach to the fuel shell. The cone penetrates almost to the center of the capsule so that the intense laser has direct access to the dense ignition region.[12−15]

The idea of a fuel capsule with a re-entrant cone is a milestone of fast ignition. Previous investigations have involved the effect of the cone angle,[16] the f number of the focusing optic and the preplasma filling inhibition of fast electron energy deposition.[17,18] It has been suggested that the target structure can collimate fast electrons[19,20] and experimental results have shown an efficient production of electrons.[21,22] To date, the detailed interaction of an intense laser with a cone target, and the precise mechanism responsible for the energy transport through the cone-shaped target is still unclear. Solid understanding of the characterization of relativistic electrons generated by a cone guiding laser pulse is essential to assess the feasibility of cone targets for full scale fast ignition conditions.

In this paper, we report the experimental studies of the interaction of an fs laser beam with a gold cone target. The laser light is optically guided by the conical geometry and focuses at the tip. he guiding effect enhances the local intensity of the laser at the cone tip. Two groups of relativistic electrons were observed on the laser propagating direction. The electron temperature increased dramatically compared to the case when a plane gold target is used.

*Project supported by the National Natural Science Foundation of China (Grant Nos. 10975121 and 11174259) and the Foundation of National Key Laboratory of Plasma Physics.

†Corresponding author. E-mail: yqgu@sina.com.cn

© 2012 Chinese Physical Society and IOP Publishing Ltd

2. Experimental setup

Experiments were carried out on the SILEX-I intense laser facility[23,24] at the Laser Fusion Research Center, China Academy of Engineering Physics (CAEP). This Ti: sapphire laser facility employed chirped-pulse-amplification (CPA) technique and maximum output was 286 TW for a 30 fs pulse duration at the wavelength of 800 nm. The contrast ratio of the laser pulses was measured to be $\sim 10^{-6}$ at 2 ns before the main pulse. Figure 1 shows a scheme of the experimental setup. An F/3 off-axis parabolic mirror focused the p-polarized 140 mm laser beam into a 10 μm circular spot (FWHM), which contained $\sim$ 12% of the laser energy at the gold cone tip. The maximum laser intensity reached 4.5×10^{19} W·cm^{-2}. The gold cone target is 1 mm long, 16 μm thick, with a 60° open angle and 10 μm diameter inner tip. Two long-focus microscopes were used to monitor the orientation of the target.

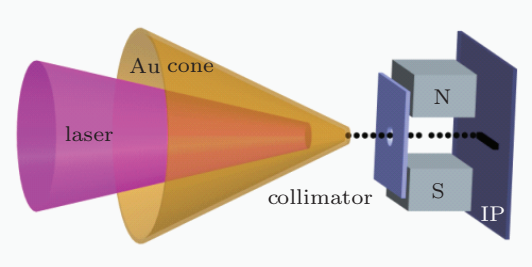


Fig. 1. (colour online) Experimental setup for intense laser interaction with a gold cone target. A gold plane target of thickness 16 μm is also used as a reference while maintaining other conditions.

The energy spectra of the relativistic electrons from the cone tip were measured by an electron spectrometer (ESM), which consists of a 1200 G permanent dipole magnet and an imaging plate (IP) (Fuji BAS-SR 2040). The entrance of the ESM is a collimator with a 5 mm aperture. The collimator is aligned with the cone tip along the laser propagating axis. The IP, covered with a 50 μm thick aluminum film to block stray laser and low energy electrons, is placed 100 mm away from the cone tip. To improve the precision of the measurement the attenuation function of IP with time is calibrated.

3. Results and discussions

For intense laser interaction with a solid target, relativistic electrons could be produced by different mechanisms such as resonance absorption, vacuum heating, and sheath inverse-bremsstrahlung. In our experiments, the ponderomotive $\boldsymbol{j}\times\boldsymbol{B}$ acceleration dominates over the hot electron generation because the laser intensity is above the relativistic intensity of 1.37×10^{18} μm^{2}W·cm^{-2}. When the relativistic electrons flow into a solid target, a return current will be induced to maintain the charge and current balance. Any conductor connected to the cone might induce an unknown influence on the transportation of the relativistic electrons. To avoid the electron return current from the target support, we used insulating glue to conglutinate the cone target on the support. Plane gold film targets of 16 μmm thick were also prepared as reference targets.

The radiated IP was scanned by the BAS-5000 reader and the raw electron signal is shown in Fig. 2. It is known that the energy of the electrons is a function of the distance from the laser axis. The typical spectra of the hot electrons are shown in Fig. 3. Relativistic electrons with energy above 2.0 MeV were observed. These electrons could be divided into two groups. Fitting the spectra with Maxwellian distribution, we can find that the effective temperatures are 200 and 934 keV respectively, while the effective temperatures of fast electrons emitted from the reference plane targets under the same laser condition are 165 and 752 keV. Considering the shot to shot difference, a 25%–40% increase of electron temperature is achieved.

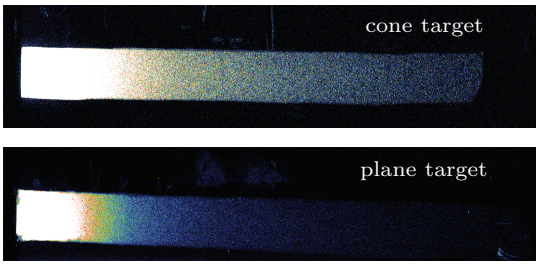


Fig. 2. (colour online) Typical comparison of the raw signal of relativistic electrons emitted from intense laser interaction with a cone gold target and a gold plane target, recorded by imaging plate.

To explore the enhancement of the electron temperature, we divide the detected hot electrons into two parts according to the position where they were generated. One part of the electrons were generated at the tip of the cone target. Due to the cone guiding effect, the laser can be reflected by the inner wall of the cone. The reflected proportion of the incident laser energy flux depends on the material and geometry of the cone. We note that 3D-PIC simulations indicate an increase in the optical intensity by more than one order of magnitude by the focusing action of the cone with an open angle of 26°.[6] In our experiments, the

focal spot consisted of a Gaussian spot with full width at half maximum (FWHM) of 10 μm (containing 12% of the total energy) and a dim ring (containing about 40% of the total energy). The laser energy in the dim ring was guided to the tip by the cone. Accordingly, the laser intensity at the cone tip are enhanced by 2–3 times. As shown in Fig. 3, an increment of 25%–40% in electron temperature, inferred from the electron spectra of the cone target compared to the plane target is consistent with the scaling law of the resonance absorption mechanism,[25] $T_e \propto I^{1/3}$ keV. The other part of the energetic electrons generated at the cone inner surface near the tip, where the laser intensity is much lower than at the cone tip. We did not detect as many low energy electrons as expected. The most likely reason is that these electrons are heated while propagating forward. The generation of a quasistatic magnetic field makes this possible. The electrons can be heated directly by the laser if a magnetic field exists.[26] In the case of the cone target, the laser light can excite an intense quasistatic magnetic field on the cone surface, which can enhance the electron energy dramatically. Therefore, optimization of the cone design and inner surface could be an avenue to improve the quality of the relativistic electron beams.

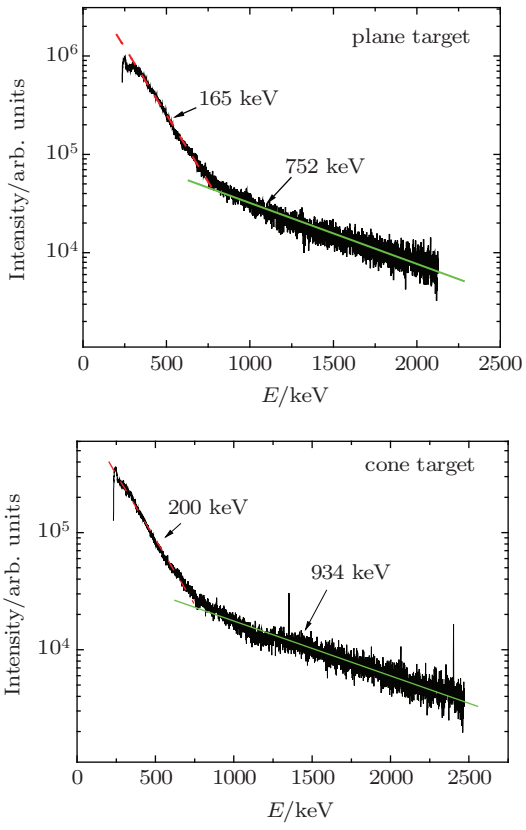


Fig. 3. (colour online) Typical comparison of the energy spectra, and the effective electron temperature of the relativistic electrons emitted from intense laser interaction with a cone gold target and a gold plane target.

4. Simulations

To reach a deeper understanding of the experiment, we carried out two-dimensional (2D) particle-in-cell (PIC) simulations. The cone guiding laser effect has been discussed in previous work.[6,14] Here, we emphasise the effect of the quasistatic magnetic field. The scales of the simulation box are $\boldsymbol{X}_L \times \boldsymbol{Y}_L = 30\,\lambda_0 \times 30\,\lambda_0$ with the time step length of 0.025 τ, the simulation duration of 50 τ and the grid size of $\Delta\boldsymbol{X} = \Delta\boldsymbol{Y} = 0.05\ \lambda_0$, where τ and λ_0 are the period and wavelength of laser pulse, respectively. A p-polarized laser pulse with a Gaussian profile in the y-direction is introduced along the axis of the cone target from the left. The laser profile in the x-direction can be described as rising up to a peak intensity in 5 τ, remaining at the peak intensity for 10 τ, and then falling to zero in another 5 τ. For the normalized amplitude of the vector potential of the incident laser, $a_0 = 5.0$ is used. The initial temperature of both the electrons and ions is 1.0 keV. The scale length of the preplasma is 1.0 λ_0 at the cone tip and the side wall. The cone is a high-Z material with a density of $20n_c$, where the effective charge-to-mass ratio is assumed to be 1/10. To note n_c is the critical density, which is related to the frequency of the laser as $n_c = m_e w_0^2/4\pi e^2$. For simplification, the normalization of the electric field and magnetic field: $E = e\hat{E}/m_e w_0 c$, $B = e\hat{B}/m_e w_0$ is used in our calculation.

While propagating inside the cone, the laser light can excite an intense quasistatic magnetic field on the cone surface. Figure 4 shows the magnetic field in z-direction (B_z) at different time. The magnetic field is most intense after 30 laser circles, and will affect the behavior of electrons in the vicinity. As mentioned above, a part of the relativistic electrons are generated at the cone inner surface near the tip. On one hand, these surface relativistic electrons are confined in the plasma skin layer and guided to the tip of the cone by pre-generated quasistatic magnetic fields. On the other hand, these hot electrons experience transverse betatron oscillations in the quasistatic magnetic fields. These oscillations are along the polarization of the laser pulse electric field, and thus an efficient energy exchange occurs when the betatron frequency is close to the laser frequency. Figure 5 shows the distribution of hot electrons above 200 keV in the cone

target. One can see the hot electrons are assembled in the cone surface and guided to the cone tip.

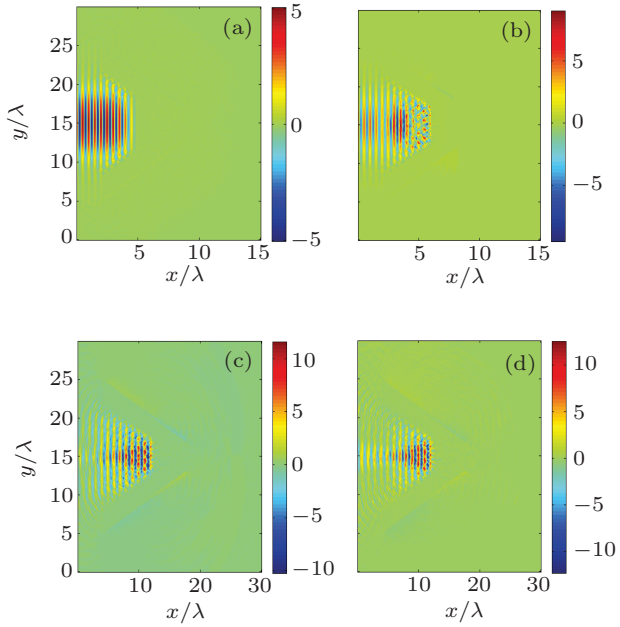


Fig. 4. (colour online) Magnetic field of z-direction in the cone at the time of 10 τ_0 (a), 20 τ_0 (b), 30 τ_0 (c), 35 τ_0 (d).

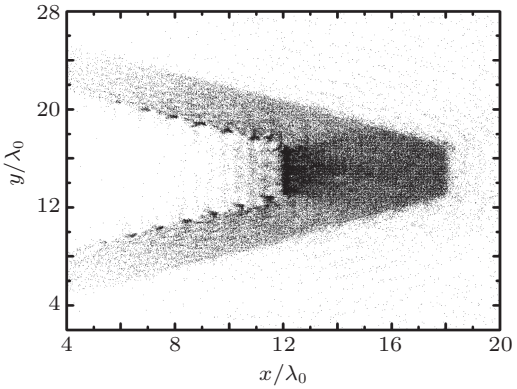


Fig. 5. The distribution of hot electrons above 200 keV in the cone target at 30 τ_0.

5. Conclusion

In conclusion, we have demonstrated the interaction of the ultra-intense laser with a cone gold target. The laser pulse is guided by the conical surface, and a 2–3 times increase of the laser intensity at the cone tip is achieved. We expect that with an optimally shaped surface it might be possible to achieve a higher concentration. The temperature of the observed electrons increased dramatically compared to the case when a plane gold target is used. It is particularly important for the fast ignition.

Acknowledgment

The authors gratefully acknowledge Prof. Wang Xiaodong, Mr. Sun Li, and Mr. Guo Yi, for operating the SILEX-I intense laser system, and Prof. Du Kai for manufacturing the gold cone targets. We also wish to thank Prof. Huang for his fruitful discussion.

References

[1] Tabak M, Hammer J, Glinsky M, Kruer W, Wilks S, Woodworth J, Campbell E and Perry M 1994 *Phys. Plasmas* **1** 1626

[2] Tanaka K, Kodama R, Mima K, Kitagawa Y, Fujita H, Miyanaga N, Nagai K, Norimatsu T, Sato T, Sentoku Y, Shigemori K, Sunahara A, Shozaki T, Tanpo M, Tohyama S, Yabuuchi T, Zheng J and Yamanaka T 2003 *Phys. Plasmas* **10** 1925

[3] Norreys P, Allott R, Clarke R, Collier J, Neely D, Rose S, Zepf M, Santala M, Bell A, Krushelnick K and Dangor A 2000 *Phys. Plasmas* **7** 3721

[4] Stephens R, Hatchett S, Turner R, Tanaka K and Kodama R 2003 *Phys. Rev. Lett.* **91** 185001

[5] Badziak J, Jablonski S and Wolowski J 2007 *Plasma Phys. Controlled Fusion* **49** B651

[6] Sentoku Y, Mima K, Ruhl H, Toyama Y, Kodama R and Cowan T 2004 *Phys. Plasmas* **11** 3083

[7] Chen Z, Kumar G, Sheng Z, Matsuoka T, Sentoku Y, Tampo M, Tanaka K, Tsutsumi T, Yabuuchi T and Kodama R 2006 *Phys. Rev. Lett.* **96** 084802

[8] Galloudec N, Humieres E, Cho B, Osterholz J, Sentoku Y and Ditmire T 2009 *Phys. Rev. Lett.* **102** 205003

[9] Chen Z, Kodama R, Nakatsutsumi M, Nakamura H, Tampo M, Tanaka K, Toyama Y, Tsutsumi T and Yabuuchi T 2005 *Phys. Rev.* E **71** 036403

[10] Yan C Y, Zhang Q J and Luo M H 2011 *Acta Phys. Sin.* **60** 391 (in Chinese)

[11] Zhou C T, He X T, Cao J M, Wang X G and Wu S Z 2009 *J. Appl. Phys.* **105** 083311

[12] Kodama R, Norreys P A, Mima K, Dangor A E, Evans R G, Fujita, Kitagawa Y, Krushelnick K, Miyakoshi T, Miyanaga N, Norimatsu T, Rose S J, Shozaki T, Shigemori K, Sunahara A, Tampo M, Tanaka K A, Toyama Y, Yamanaka T and Zepf M 2001 *Nature* **412** 798

[13] Kodama R, Mima K, Tanaka K, Kitagawa Y, Fujita H, Takahashi K, Sunahara A, Fujita K, Habara H, Jitsuno T, Sentoku Y, Matsushita T, Miyakoshi T, Miyanaga N, Norimatsu T, Setoguchi H, Sonomoto T, Toyama Y and Yamanaka T 2001 *Phys. Plasmas* **8** 2268

[14] Zhou C, He X and Yu M 2008 *Appl. Phys. Lett.* **92** 151502

[15] Cao L, Yu W, Yu M, Xu H, He X, Gu Y, Liu Z, Li J and Zheng C 2008 *Phys. Rev.* E **78** 036405

[16] Nakatsutsumi M, Kodama R, and Norreys P, Awano S, Nakamura H, Norimatsu T, Ooya A, Tampo M, Tanaka K, Tanimoto T, Tsutsumi T and Yabuuchi T 2007 *Phys. Plasmas* **14** 050701

[17] Baton S, Koenig M, Fuchs J, Benuzzi-Mounaix A, Guillou P, Loupias B, Vinci T, Gremillet L, Rousseaux C, Drouin M, Lefebvre E, Dorchies F, Fourment C, Santos J, Batani

D, Morace A, Redaelli R, Nakatsutsumi M, Kodama R, Nishida A, Ozaki N, Norimatsu T, Aglitskiy Y, Atzeni S and Schiavi A 2008 *Phys. Plasmas* **15** 042706

[18] Woerkom L V, Akli K U, and Bartal T, Beg F N, Chawla S, Chen C D, Chowdhury E, Freeman R R, Hey D, Key M H, King J A, Link A, Ma T, Mackinnon A J, MacPhec A G, Offermann D, Ovchinnikov V, Patel P K, Schumacher D W, Stephens R B and Tsui Y Y 2008 *Phys. Plasmas* **15** 056304

[19] Robinson A P and Sherlock M 2007 *Phys. Plasmas* **14** 083105

[20] Lei A, Cao L, Yang X, Tanaka K, Kodama R, He X, Mima K, Nakamura T, Norimatsu T, Yu W and Zhang W 2009 *Phys. Plasmas* **16** 020702

[21] Kodama R, Tanaka K A, Sentoku Y, Matsushita T, Takahashi K, Fujita H, Kitagawa Y, Kato Y, Yamanaka T and Mima K 2000 *Phys. Rev. Lett.* **84** 674

[22] Yu W, Bychenko V, Sentoku Y, Yu M, Sheng Z and Mima K 2000 *Phys. Rev. Lett.* **85** 570

[23] Liu H J, Gu Y Q, Zheng Z J, Jiao C Y, Nam S M, Han Z M, Wang X X, He Y L, Wen T S, Zhang S G, Wen X L, Zhou K N, Wang X D, Huang X J and Hua J F 2006 *Chin. Phys. Lett.* **23** 1527

[24] Peng H, Huang X, Zhu Q, Zhou K, Wei X, Zeng X, Liu L, Wang X, Guo Y, Lin D, Xu B, Chu X and Zhang X 2006 *Laser Phys.* **16** 1

[25] Beg F N, Bell A R, Dangor A E and Danson C N 1997 *Phys. Plasmas* **4** 447

[26] Pukhov A, Sheng Z M and Meyer-ter-vehn J 1999 *Phys. Plasmas* **6** 2847